2024-02-01

Spatiotemporal variations in reef manta ray (Mobula alfredi) residency at a remote meso-scale habitat and its importance in future spatial planning

Harris, J

10.1002/aqc.4089
Aquatic Conservation: Marine and Freshwater Ecosystems
Wiley

Received: 20 October 2023 | Revised: 29 December 2023 | Accepted: 30 December 2023

DOI: 10.1002/aqc.4089

RESEARCH ARTICLE

WILEY

Spatiotemporal variations in reef manta ray (*Mobula alfredi*) residency at a remote meso-scale habitat and its importance in future spatial planning

Joanna L. Harris[1,2] | Phil Hosegood[2] | Clare B. Embling[2] | Benjamin J. Williamson[3] | Guy M. W. Stevens[1]

[1]Manta Trust, Corscombe, UK

[2]School of Biological and Marine Sciences, University of Plymouth, Plymouth, UK

[3]UHI North, West and Hebrides, University of the Highlands and Islands, Thurso, UK

Correspondence
Joanna L. Harris, The Manta Trust, Catemwood House, Norwood Lane, Corscombe, Dorset, DT2 0NT, UK.
Email: joanna.l.harris@plymouth.ac.uk

Funding information
This work was supported by the Bertarelli Foundation and the Garfield Weston Foundation

Abstract

1. The Chagos Archipelago's vast no-take marine protected area (MPA, 640,000 km^2) provides refuge for elasmobranchs facing unsustainable depletion by fisheries. Nonetheless, illegal, unreported and unregulated (IUU) fishing poses a substantial threat, and potential future changes to the use of the MPA could render elasmobranchs increasingly vulnerable to exploitation, putting geographically isolated populations, such as reef manta rays (*Mobula alfredi*) at risk of local extinction. Therefore, the species' long-term movements and habitat use must be identified to help prioritize current enforcement activity and inform future spatial planning.
2. Passive acoustic telemetry and modelled environmental data were used to investigate variations in 42 tagged *M. alfredi* utilization of a meso-scale aggregation hotspot, Egmont Atoll, between 2019 and 2022.
3. *Mobula alfredi* displayed the highest levels of residency ever reported (77%), with prolonged absences (>2 months) limited to seven individuals. Egmont atoll was used year-round, with activity peaks during the southeast monsoon (April – November), particularly at sites on the southwest, while sites on the northwest were predominately frequented in the northwest monsoon (December–March). Tags were most likely to be detected when the Indian Ocean Dipole (IOD) was in a positive phase with a greater mixed layer depth, associated with a depression of chlorophyll α levels in the Indian Ocean. Thus, *M. alfredi* may be particularly reliant on Egmont Atoll, where they are predominantly observed feeding, when prey resources are limited elsewhere.
4. In a region where the threat of fisheries is of increasing concern, the identification of crucial *M. alfredi* habitats is essential for conservation management planning. Given the significant role of Egmont Atoll for the local population, regular IUU enforcement patrols are crucial, particularly during the southeast monsoon. Any future changes to the MPA should prioritize preserving and actively enforcing no-take regulations at Egmont Atoll.

KEYWORDS
acoustic telemetry, elasmobranch, IUU fishing, marine protected area, *Mobula alfredi*, residency

1 | INTRODUCTION

The marine environment is under unprecedented pressure from ever-increasing exploitation (Crowder et al., 2008; Silber et al., 2017), with many marine species being driven towards extinction. Of particular concern are those whose recovery is hindered by their conservative life-history traits, including slow growth, late maturation and low fecundity, such as elasmobranchs (Collins, Nuno, Benaragama, et al., 2021; Collins, Nuno, Broderick, et al., 2021; Dulvy, Fowler, et al., 2014; Fernando & Stewart, 2021; Stevens, 2016; Ward-Paige et al., 2013). Many species are also under pressure from a multitude of other anthropogenic threats, including human-induced climate change, unregulated tourism, development and habitat degradation (Carpenter et al., 2023; Harris et al., 2020; Murray et al., 2019; Rohner et al., 2013; Stevens & Froman, 2018; Venables et al., 2016).

In the Chagos Archipelago, elasmobranchs are legally protected from both targeted fisheries and most other anthropogenic threats as the region is predominantly undeveloped and encompassed by a vast (640,000 km^2) no-take marine protected area (MPA) with on-site enforcement (Hays et al., 2020; Sheppard et al., 2012). Nonetheless, illegal, unreported, and unregulated (IUU) fishing is a common issue, particularly for sharks and rays that are heavily targeted (Clark et al., 2015; Collins, Nuno, Broderick, et al., 2021; Curnick et al., 2021; Hays et al., 2020; Tickler et al., 2019). Estimates suggest up to 15,000 individual sharks are illegally caught per year across the Chagos Archipelago (Ferretti et al., 2018). Data on rays is currently limited to a single study that reviewed IUU photographic archives and found an estimated 20 tonnes of mobulid rays on just seven illegal fishing vessels (Harris & Stevens, in review). However, as only around 10% of IUU in the MPA is detected (Jacoby et al., 2020; Price et al., 2010) and due to the lack of systematic reporting and species-specific data (Collins, Nuno, Broderick, et al., 2021; Ferretti et al., 2018; Harris et al., in review), this is likely a vast underestimation (Harris & Stevens, in review).

Despite IUU, the current level of protection in the Chagos Archipelago provides essential refuge for many species (Andrzejaczek et al., 2020; Carlisle et al., 2019; Harris, 2019). However, the establishment of this MPA has faced legal challenges from the Mauritian government amid an ongoing sovereignty dispute with the UK government over the archipelago (Strating, 2023). Mauritius contends that the MPA encroaches upon their fishing rights, thereby violating international law, and asserts that it should be revoked and replaced with a new agreement that includes an MPA that is spatially planned by Mauritius (Strating, 2023). Any changes to the MPA could increase the susceptibility of elasmobranchs to target and non-targeted fisheries throughout the region as well as other pressures that threaten the species throughout the Indian Ocean. For example, boat strikes and propeller injuries if there is an increase in boat traffic (Strike et al., 2022) and damage from anthropogenic activities that degrade habitats, such as anchoring on coral reefs or their intentional destruction to allow boat access (Harris et al., 2020). One such species is the reef manta ray (*Mobula alfredi*), a zooplanktivorous elasmobranch species of the monogeneric Mobulidae family (mobulids) (Hosegood et al., 2020; Marshall et al., 2009; Notarbartolo di Sciara et al., 2020; White et al., 2017). Reported *M. alfredi* populations throughout their Indo-West Pacific range are small (typically a few hundred), geographically fragmented and often isolated (Couturier et al., 2012; Hosegood et al., 2020; Humble et al., 2023; Kashiwagi et al., 2011; Whitney et al., 2023). Many of these populations have faced declines, predominantly driven by targeted and non-targeted fisheries (Rohner et al., 2013; Rohner et al., 2017; Ward-Paige et al., 2013). As one of the least fecund of all elasmobranchs, with the lowest intrinsic rate of population increase (Dulvy et al., 2017), this declining trend will likely lead to local extinctions (Dulvy, Pardo, et al., 2014; Marshall et al., 2022). To mitigate the risk of fishing pressure in the Chagos Archipelago it is essential to understand how *M. alfredi* utilizes the marine environment on multiple spatial scales to help prioritize current enforcement activity and inform future spatial planning.

Investigation into the broadscale (>100 km) movements of *M. alfredi* in the region using acoustic and satellite telemetry has shown that the species migrate widely throughout the archipelago but remain within the boundary of the MPA (Andrzejaczek et al., 2020; Harris, 2019). Stable isotope analysis supports these findings and indicates that individuals make frequent migrations between the atolls (Harris et al., 2023). However, these studies do not provide sufficient evidence for targeted management, for example, locations that should be prioritized for enforcement patrols. Conversely, while a study of fine-scale (<1 km) of *M. alfredi* habitat, Manta Alley, Egmont Atoll, helped to identify when aggregations were likely to occur (Harris et al., 2021), which could be used for targeted management, it does not take into account the potential network of important habitats that likely exist nearby, similar to other *M. alfredi* populations (Harris & Stevens, 2021). Based on the regularity that *M. alfredi* utilizes Egmont Atoll in the southwest of the Chagos Archipelago, the atoll has been identified as a key habitat for the species (Harris, 2019; Harris et al., 2021). This meso-scale (30 km^2) atoll has the highest documented *M. alfredi* activity in the region (Harris et al., 2023). Therefore, there is an urgent need for a more detailed understanding of the spatial and temporal dynamics of *M. alfredi* utilization of this habitat to inform and develop current and future protection strategies.

Here, passive acoustic telemetry and modelled environmental data were used to investigate *M. alfredi* use of Egmont Atoll to identify annual and seasonal variations in visitation patterns and the intensity at which the location is utilized and assess the environmental factors that influence visitation patterns. This knowledge will enhance our current

understanding of the *M. alfredi* population's ecology and movements in the Chagos Archipelago and highlight areas of particular concern that should be prioritized for current enforcement activity or future spatial planning should the MPA be repurposed.

2 | METHODS

2.1 | Study location

Egmont Atoll, situated in the southwest of the Chagos Archipelago (Figure 1), has an interior lagoon system that is partially separated from the open ocean by reef crests and flats, with narrow connecting channel systems (Harris et al., 2021). Multiple *M. alfredi* aggregation sites are located around the atoll (Table 1), which include foraging hotspots and cleaning stations (Harris et al., 2021).

2.2 | Season classification

The Chagos Archipelago has two seasons, which can be characterized by the reversal of southeast and northwest winds [hereafter, the southeast (SE) monsoon and northwest (NW) monsoon, respectively]. However, the months these monsoons occur vary in the literature (e.g., Bovalo & Barthe, 2012; Sheppard et al., 1999; Williamson et al., 2020). Therefore, in the current study, the seasons were broadly identified following Harris et al. (2020) and Anderson et al. (2011) using hourly wind direction data (2010–2020) obtained from Meteoblue AG, Basel, Switzerland (www.meteoblue.com). These data were used to calculate the monthly wind direction as the percentage of days in a month that the wind direction was predominantly south-easterly (SE monsoon; 101.3–168.8°) and north-westerly (NW monsoon; 281.3–348.8°). Each month was then classified as either SE or NW monsoon based on the highest monthly percentage of each direction.

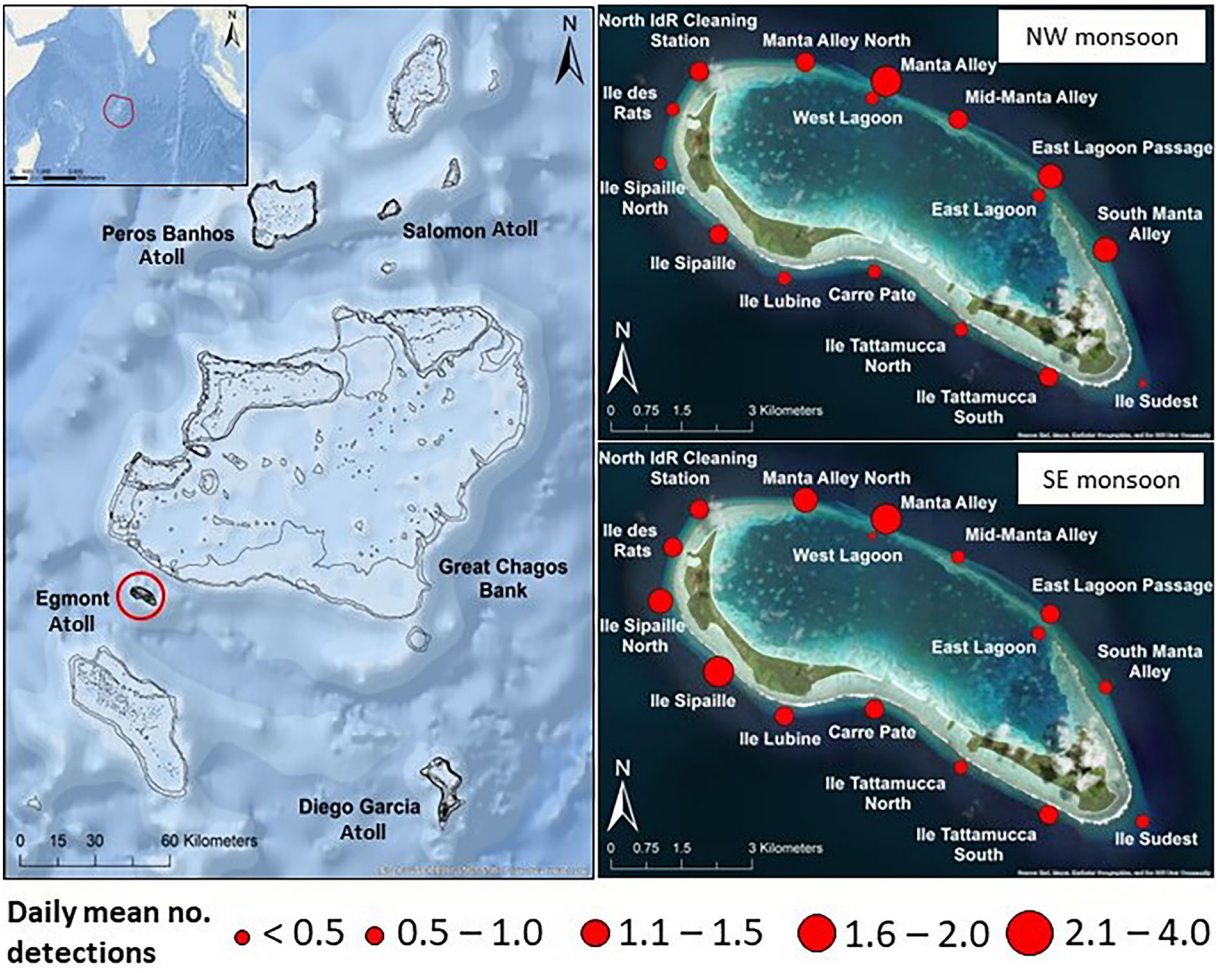

FIGURE 1 The Central Indian Ocean with the Chagos Archipelago vast (640,000 km^2) no-take marine protected area indicated within the red line (left inset). The Chagos Archipelago with Egmont Atoll indicated within the red circle (left). Egmont Atoll acoustic receiver locations (red dots) during the northwest monsoon (top right), and the southeast monsoon (bottom right). The size of the red dots corresponds to the daily mean number of detections per tagged reef manta ray (*Mobula alfredi*) that occurred at each location during each season calculated from the total number of detections that occurred each day/the total number of active tags each day from which a seasonal mean was calculated.

TABLE 1 Summary of *Mobula alfredi* acoustic tag deployments ($n = 42$), tracking, detections and residency index (I_R) at Egmont Atoll.

Manta ID	Tag ID	Sex	Maturity	Deployment date	Date of first detection	Date of last detection	No. tracking days	No. detection days	Max no. consecutive detection days	No. times absent from the array (>1 day)	Max consecutive days of absence	Residency index (I_R)
CG-MA-0142	18884	F	Juvenile	02/12/2019	03/12/2019	29/10/2020	333	276	161	25	7	82.9%
CG-MA-0124	18885	M	Adult	20/11/2019	21/11/2019	08/02/2021	446	358	187	32	14	80.3%
CG-MA-0128	18886	F	Juvenile	21/11/2019	08/05/2020	14/03/2022	844	83	31	11	543	9.8%
CG-MA-0117	18887	F	Juvenile	20/11/2019	22/11/2019	02/12/2020	378	302	92	29	11	79.9%
CG-MA-0161	18888	M	Adult	02/12/2019	04/12/2019	27/12/2019	25	7	2	5	8	28.0%
CG-MA-0141	18889	F	Adult	28/11/2019	02/12/2019	20/01/2020	53	31	16	9	3	58.5%
CG-MA-0035	18890	F	Juvenile	20/11/2019	20/11/2019	09/12/2020	385	361	193	14	6	93.8%
CG-MA-0070	18891	F	Juvenile	01/12/2019	01/12/2019	04/01/2021	400	297	122	44	11	74.3%
CG-MA-0046	18892	F	Adult	25/11/2019	03/12/2019	19/02/2022	817	201	24	96	111	24.6%
CG-MA-0112	18893	M	Juvenile	01/12/2019	01/12/2019	30/09/2020	304	240	157	23	7	78.9%
CG-MA-0094	18894	F	Juvenile	30/11/2019	30/11/2019	05/06/2021	553	503	179	32	4	91.0%
CG-MA-0125	18895	M	Juvenile	20/11/2019	20/11/2019	15/02/2021	453	209	38	35	109	46.1%
CG-MA-0151	18896	M	Adult	01/12/2019	08/12/2019	04/05/2021	521	349	57	31	67	67.0%
CG-MA-0088	18897	M	Juvenile	28/11/2019	01/12/2019	08/08/2020	254	174	91	28	12	68.5%
CG-MA-0140	18898	M	Juvenile	30/11/2019	30/11/2019	04/07/2020	217	112	45	27	36	51.6%
CG-MA-0139	18899	F	Adult	25/11/2019	04/12/2019	28/08/2020	277	237	157	22	8	85.6%
CG-MA-0118	18900	M	Juvenile	19/11/2019	19/11/2019	13/05/2020	176	92	24	25	22	52.3%
CG-MA-0119	18901	F	Juvenile	19/11/2019	20/11/2019	08/12/2020	385	291	182	26	11	75.5%

TABLE 1 (Continued)

Manta ID	Tag ID	Sex	Maturity	Deployment date	Date of first detection	Date of last detection	No. tracking days	No. detection days	Max no. consecutive detection days	No. times absent from the array (>1 day)	Max consecutive days of absence	Residency index (I_R)
CG-MA-0120	18902	F	Juvenile	19/11/2019	20/11/2019	21/11/2019	2	2	N/A		N/A	N/A
CG-MA-0121	18903	M	Juvenile	19/11/2019	20/11/2019	12/02/2021	451	416	165	19	5	92.2%
CG-MA-0214	50909	M	Adult	01/12/2021	01/12/2021	14/03/2022	103	103	97	0	1	100.0%
CG-MA-0192	50910	F	Juvenile	12/04/2021	12/04/2021	09/02/2022	303	88	20	20	176	29.0%
CG-MA-0171	50911	M	Adult	13/04/2021	13/04/2021	22/04/2021	10	10	10	0	0	100.0%
CG-MA-0194	50912	F	Juvenile	13/04/2021	13/04/2021	19/06/2021	67	28	9	4	35	41.8%
CG-MA-0146	50913	M	Juvenile	13/04/2021	13/04/2021	02/05/2021	19	19	14	1	1	100.0%
CG-MA-0081	50914	F	Juvenile	10/04/2021	10/04/2021	11/04/2021	2	2	N/A		N/A	N/A
CG-MA-0096	50915	M	Adult	13/04/2021	14/04/2021	08/08/2021	117	116	67	1	1	99.1%
CG-MA-0037	50916	F	Adult	12/04/2021	12/04/2021	08/05/2021	27	27	27	0	0	100.0%
CG-MA-0153	50917	F	Adult	12/04/2021	12/04/2021	08/12/2021	240	200	101	3	37	83.3%
CG-MA-0186	50918	M	Adult	13/04/2021	13/04/2021	19/10/2021	189	57	23	3	71	30.2%
CG-MA-0093	50919	F	Adult	01/12/2021	01/12/2021	09/02/2022	70	69	64	1	231	98.6%
CG-MA-0208	50920	M	Juvenile	13/04/2021	13/04/2021	26/08/2021	135	135	101	1	1	100.0%
CG-MA-0166	57692	F	Juvenile	11/03/2020	15/03/2020	27/10/2020	230	190	42	22	7	82.6%
CG-MA-0168	57694	F	Adult	13/03/2020	13/03/2020	07/04/2020	26	26	26	0	0	100.0%
CG-MA-0163	57695	F	Juvenile	11/03/2020	12/03/2020	26/02/2021	352	349	319	3	1	99.1%
CG-MA-0164	57696	F	Adult	11/03/2020	13/03/2020	27/02/2021	353	346	178	5	3	98.0%

(Continues)

TABLE 1 (Continued)

Manta ID	Tag ID	Sex	Maturity	Deployment date	Date of first detection	Date of last detection	No. tracking days	No. detection days	Max no. consecutive detection days	No. times absent from the array (>1 day)	Max consecutive days of absence	Residency index (I_R)
CG-MA-0080	57697	M	Juvenile	11/03/2020	11/03/2020	19/07/2020	130	116	72	8	4	89.2%
CG-MA-0054	57698	F	Juvenile	12/03/2020	12/03/2020	12/11/2020	246	239	193	4	4	97.2%
CG-MA-0170	57699	F	Juvenile	13/03/2020	13/03/2020	04/09/2020	175	171	64	4	2	97.7%
CG-MA-0037	57700	F	Adult	12/03/2020	12/03/2020	26/03/2020	15	15	15	0	0	100.0%
CG-MA-0167	57702	F	Juvenile	12/03/2020	12/03/2020	11/04/2020	30	30	29	1	1	100.0%
CG-MA-0169	57703	F	Juvenile	13/03/2020	13/03/2020	31/08/2020	171	171	91	1	1	100.0%

2.3 | Acoustic telemetry

Between November 2019 and March 2022, VR2W-69 kHz omnidirectional acoustic receivers [InnovaSea Systems, Inc. (Vemco Inc.)] were deployed at a total of 16 sites (Figure 1 and Table 2). The utility function of each site (cleaning station or feeding area) was determined by the predominant (≥50%) *M. alfredi* activity observed during in-water observations at the location (Table 2). Feeding and cleaning behaviour were identified based on feeding or cleaning activities as described by Stevens (2016). The initial acoustic array was established in November 2019 and consisted of five acoustic receivers (Harris et al., 2021). In March 2020, the array was extended to 14 receivers at a mean spatial interval of 2 km around the outer rim of Egmont Atoll. All receivers were deployed at depths ranging from 2 to 48 m above the seabed in waters between 10 and 65 m on the reef flat close to the reef slope. The data was downloaded, and the array was serviced in April 2021. Due to logistical constraints, the receivers at East Lagoon Passage and Manta Alley had to be relocated approximately 200 m shoreward; these locations were named East Lagoon and West Lagoon, respectively. The data from all receivers were downloaded again in March 2022. The receiver at Ile Sudest and Ile Sipaille North could not be recovered, and the receiver at Ile Lubine stopped recording in October 2021. Acoustic tags were detected within approximately 160 m of the receivers: mean = 162 ± 31 m (*SD*, *n* = 14) as determined by range testing (Harris et al., 2021). Due to the remoteness of Egmont Atoll and the logistical challenges of working in the region, range testing could not be compared under different environmental conditions.

During the same period, a total of 42 Innovasea (Vemco) V16-4x acoustic transmitter tags [InnovaSea Systems, Inc. (Vemco Inc.)] were deployed on 26 females (adults = 9, juvenile = 17) and 16 males (adults = 7, juvenile = 9) *M. alfredi* (Table 1) using a modified Hawaiian hand sling while freediving. All tags were tethered to a titanium anchor (Wildlife Computers) with a small diameter stainless steel cable and programmed to transmit a unique acoustic signal at random intervals between 30 and 90 s at 69 kHz. Before being tagged, each individual's unique ventral spot pattern was photographed for identification, and their sex and visually estimated size class, which acts as a proxy for maturity, were recorded. Sex and maturity in males were determined by the presence of claspers, which are not present in females (Stevens, 2016). Males with completely calcified claspers that extended past the pelvic fins were deemed mature (Stevens, 2016). Females were deemed mature if they were visibly pregnant, if they had mating wounds or scars or if they had a disc width greater than 320 cm (Stevens, 2016). All activities were approved by the University of Plymouth Animals in Science Ethics Committee under permits ETHICS-24-2019 and ETHICS-37-2020.

2.4 | Acoustic data analysis

All tag detection data were imported into VUE software (version 2.8.1) and filtered for active tags. The false detection analyser was

TABLE 2 Summary of acoustic receiver deployment sites

Site Name	Seasonality (monsoon)	Site description	Predominant site function and % of observation	Deployed (start date)	Retrieved (end date)	Total no. days recording	No. days recording (NW monsoon)	No. days recording (SE monsoon)	No. of tags detected	Mean resident event (mean min ± SD)	Max resident event (min)
North IdR Cleaning Station*	None	Coral bommie at 10 m close to drop-off	Cleaning Station (92%, $n = 90$)	19/11/2019	10/03/2022	841	347	494	36	25 ± 40	436
Manta Alley North*	SE	Shallow (<15 m) close to drop off and narrow lagoon inlet	Feeding area (100%, $n = 5$)	11/03/2020	07/03/2022	729	246	483	37	26 ± 44	429
Manta Alley	None	Outside a narrow (<350 m) shallow (<5 m) lagoon inlet. Location depth approximately 65 m	Feeding area (90%, $n = 86$)	30/11/2019	10/04/2021	507	243	264	30	30 ± 51	586
West Lagoon	None	Within shallow (<10 m) lagoon inlet	Feeding area (98%, $n = 53$)	11/04/2021	14/03/2022	335	104	231	13	14 ± 26	166
Mid-Manta Alley*	NW	Shallow (<15 m) close to drop-off	Feeding area (86%, $n = 14$)	11/03/2020	12/03/2022	729	246	483	39	18 ± 30	268
East Lagoon Passage	NW	Shallow (<15 m) located at the ocean end of a very narrow (<30 m), shallow (<5 m) lagoon inlet	Feeding area (91%, $n = 44$)	11/03/2020	02/04/2021	395	142	253	26	18 ± 29	277
East Lagoon	None	Shallow (<10 m) located at the lagoon end of a very narrow (<30 m), shallow (<5 m) lagoon inlet	Feeding area (91%, $n = 44$)	12/04/2021	14/03/2022	334	104	230	11	21 ± 39	211
South Manta Alley*	NW	Shallow (<15 m) close to drop off and narrow lagoon inlet	Feeding area (100%, $n = 20$)	30/11/2019	13/03/2022	841	347	494	41	16 ± 26	294
Ile Sudest	SE	Shallow (<15 m) reef flat	Unknown	01/12/2019	16/03/2021	507	243	264	25	15 ± 27	197
Ile Tattamucca North*	SE	Shallow (<15 m) steep rocky slope	Feeding area (100%, $n = 6$)	11/03/2020	14/03/2022	729	246	483	33	13 ± 25	262
Ile Tattamucca South*	SE	Shallow (< 15 m) steep rocky slope	Feeding area (100%, $n = 6$)	11/03/2020	13/03/2022	729	246	483	35	23 ± 37	307
Carre Pate*	SE	Shallow (<10) sandy bay	Feeding area (100%, $n = 6$)	11/03/2020	11/03/2022	729	246	483	35	20 ± 33	287
Ile Lubine	SE	Shallow (<10 m) reef flat close to drop-off	Feeding area (100%, $n = 30$)	11/03/2020	19/10/2021	729	246	483	31	23 ± 35	359

(Continues)

TABLE 2 (Continued)

Site Name	Seasonality (monsoon)	Site description	Predominant site function and % of observation	Deployed (start date)	Retrieved (end date)	Total no. days recording	No. days recording (NW monsoon)	No. days recording (SE monsoon)	No. of tags detected	Mean resident event (mean min ± SD)	Max resident event (min)
Ile Sipaille*	SE	Shallow (< 15 m) reef flat close to drop-off	Feeding area (99%, $n = 67$)	19/11/2019	07/03/2022	841	347	494	39	21 ± 34	323
Ile Sipaille North	SE	Shallow (< 15 m) reef flat close to drop-off	Feeding area (99%, $n = 37$)	11/03/2020	11/04/2021	395	142	253	25	18 ± 29	227
Ile des Rats*	SE	Shallow (<10 m) reef flat close to drop-off	Feeding area (98%, $n = 51$)	11/03/2020	12/03/2022	729	246	483	36	17 ± 27	195

Note: Total recording duration (days) is followed by the number of days each acoustic receiver was recording during the NW and SE monsoons, as identified in the current study. Site names followed by an asterisk (*) indicate those that were active throughout Period 2 (11 March 2020 to 11 April 2021) and Period 3 (12 April 2021 to 14 March 2022). Predominant site function shows the function of the site followed by the percentage of in-water observations where this behaviour was recorded in parentheses.

then applied to identify false detections, using a ratio of short (<30 min) and long (>12 h) periods between detections calculated from the time between detections on each receiver (Harris et al., 2021; Simpfendorfer et al., 2015). All detections that appeared to be false were removed from further analysis.

Overall residency of individuals to Egmont Atoll, a residency index (I_R), was calculated using the following formula (Afonso et al., 2008; Harris & Stevens, 2021), modified to begin the detection period from the date of deployment rather than the date of the first detection. Results range from 0% (no residency) and 100% (absolute residency). While there are other formulas that can be used to calculate residency, this one was chosen as it allowed comparison with other studies that used the same approach (Appert et al., 2023). To reduce bias associated with a low number of tracking days, tags with track lengths <7 days were excluded from I_R analysis.

$$I_R = \frac{\text{Number of days detected}}{\text{Number of days from deployment to last detection} + 1} \times 100$$

Variations in visitation patterns were investigated in terms of tag detections and resident events [Vtrack R package (Campbell et al., 2012) in R 4.2.2 (R Core Team, 2023)]. A resident event was identified when two or more consecutive detections occurred within 60 minutes at a single receiver and concluded at the time of the last detection when no further detections occurred in that timeframe or when the tag was detected by another receiver (Harris et al., 2021). When a tag was not detected on the acoustic array for >1 day, the individual was considered absent from Egmont Atoll. The total number and duration of absences for each tagged *M. alfredi* was calculated. Absences were classified as extended if they were above the average duration for all individuals.

To reduce bias that may arise from the fluctuating number of active tags due to staggered deployment and various tag retention times, subsequent analysis was based on the daily number of active tags, including those with track lengths <7 days (Table 1). The daily number of active tags was calculated from the cumulative daily number of tags deployed minus the cumulative daily number of tags lost. A tag was considered active from the date of deployment and lost after the last recorded detection as of the most recent data download (March 2022). The last recorded detection is a conservative estimate of tag retention time as *M. alfredi* sometimes emigrate away from areas for long periods. For example, at Egmont Atoll, a tag that was thought to have failed as no detections occurred between its deployment in November 2019 and when data were downloaded in March 2020 (Harris et al., 2021) was subsequently detected 169 days later (Table 1).

A Welch's ANOVA was used to investigate whether the daily mean number of detections and daily mean resident event duration per tagged *M. alfredi* (number of detections a day or total daily resident event duration a day/the number of active tags on that day) varied for the whole of Egmont Atoll and/or at each individual site by demographics, seasons and years. To investigate whether resident events varied by demographics at each site, a Welch's ANOVA was used to compare overall mean resident event duration at each of the

16 locations by sex and maturity. For seasonal analysis, the daily mean number of detections and daily mean resident event durations per tagged *M. alfredi* between the SE and NW monsoon (daily mean number of detections or daily mean resident event durations per tagged *M. alfredi* / total number of days in SE or NW monsoon) were compared. For annual analysis, detection data were divided into three periods: Period 1 = 19 November 2019 to 10 March 2020, Period 2 = 11 March 2020 to 11 April 2021 and Period 3 = 12 April 2021 to 14 March 2022, due to the variation in number and locations of acoustic receivers (Table 2). The daily mean number of detections per tagged *M. alfredi* and the daily mean resident event durations were then compared between Periods 2 and 3 [daily mean number of detections or daily mean resident event durations per tagged *M. alfredi*/total number of days in Period 2 or 3 (Period 1 was excluded as only five acoustic receivers were active for 4 months)]. A Welch's ANOVA was applied to only the detections recorded by acoustic receivers that were continuously active during both periods ($n = 9$, Table 1).

2.5 | Boosted regression trees

The relationship between environmental variables and visitation patterns of tagged *M. alfredi* to Egmont Atoll was investigated using boosted regression trees (BRT). BRT is an advanced machine learning technique that constructs and combines numerous relatively simple decision trees in succession to fit the residuals from each preceding tree (Elith et al., 2008). This modelling technique circumvents autocorrelation by randomly selecting (without replacement) a proportion of the data at each iteration and has several other advantages, such as being able to fit complex, nonlinear relationships, model interactions between response variables and not requiring assumptions about the residuals of the model (Derville et al., 2016; Elith et al., 2008).

Model results provide the relative importance of predictor variables calculated by averaging the frequency with which a variable is selected for splitting and the squared improvement resulting from these splits (Elith et al., 2008), which is then scaled 100% across all the variables (Elith et al., 2008). Predictor variables with higher percentages suggest a greater effect on the response variable (Elith et al., 2008).

The response variable was the daily mean number of detections per tagged *M. alfredi* recorded by all acoustic receivers from 11 March 2020 to 11 March 2021 (365 days), which had the most comprehensive spatial coverage of the atoll. Six predictor variables (Table 3) that have been suggested to influence *M. alfredi* occurrence in the region were included: moon phase, ocean current direction and speed, sea surface temperature (SST), mixed layer depth (MLD) and the Indian Ocean Dipole (IOD) (Harris, 2019; Harris et al., 2023, 2021; Harris & Stevens, 2021; Robinson et al., 2023; Stevens, 2016).

Daily fraction of the moon that was illuminated was obtained from the United States Naval Observatory (https://aa.usno.navy.mil/data/MoonPhases). Daily current direction, current speed, SST and MLD were obtained for Egmont Atoll from Copernicus Marine Service's

TABLE 3 Description of predictor variables included in boosted regression trees analysis of the daily mean number of detections per tagged *Mobula alfredi* recorded by all acoustic receivers at Egmont from 11 March 2020 to 11 March 2021 (365 days) are described.

Predictor No.	Predictor	Unit	Mean	Description
1	Mixed layer depth	m	19.7	Depth at which the density increases by 0.1 kg m^3 (0.2°C) relative to 10 m below the surface extracted from Copernicus Marine Service's MyOcean Viewer (https://marine.copernicus.eu/access-data/myocean-viewer).
2	Moon phase	%	0.5	Daily fraction of the moon that was illuminated obtained from the United States Naval Observatory (https://aa.usno.navy.mil/data/MoonPhases).
3	Current speed	$m.s^{-1}$	0.24	Daily depth-mean (50 m) calculated eastward (*u*) and northward (*v*) components extracted from Copernicus Marine Service's MyOcean Viewer (https://marine.copernicus.eu/access-data/myocean-viewer).
4	Current direction	°(N)	182.10	Daily depth mean (50 m) calculated eastward (*u*) and northward (*v*) components extracted from Copernicus Marine Service's MyOcean Viewer (https://marine.copernicus.eu/access-data/myocean-viewer).
5	Temperature	°C	28.40	Daily depth-mean (50 m) calculated from data extracted from Copernicus Marine Service's MyOcean Viewer (https://marine.copernicus.eu/access-data/myocean-viewer).
6	Dipole Mode Index (DMI)	°C	0.02	Weekly difference between the southeastern and western tropical Indian Ocean SST anomalies (Saji & Vinayachandran, 1999) obtained from the Bureau of Meteorology, Australia [Climate monitoring graphs (bom.gov.au)] and linearly interpolated into a daily time scale.

Note: Mean values are those that are maintained for partial dependency and interaction plots.

MyOcean Viewer (https://marine.copernicus.eu/access-data/myocean-viewer). For ocean current data, eastward (*u*) and northward (*v*) components were extracted, and a depth mean was calculated for the top 65 m of the water column, corresponding to the maximum MLD observed, and then converted to current direction (°) and current speed ($m \cdot s^{-1}$). SST was also calculated as a 65 m depth mean. Daily MLD was estimated as the depth at which the density increases by 0.1 kg m^3 (0.2°C) relative to 10 m below the surface. This is a highly conservative modelling method leading to shallow MLD estimates due to weak stratification in the mixed layer; therefore, it was validated by manually establishing the depth of the thermocline using binned temperature profiles whereby the depth bin at which the temperature was 1°C lower than the temperature at 10 m depth was considered the thermocline. The 1°C threshold was chosen based on *in situ* CTD profiles acquired during multiple research expeditions under a range of environmental conditions. The model and manual estimates of MLD were highly correlated (rho = 0.74, $p < 0.001$); therefore, modelled data were deemed to accurately reflect temporal changes in MLD and sufficient for further analysis. The IOD [an ocean–atmosphere interaction, which cycles through active (positive and negative) and neutral phases] is measured by the dipole mode index (DMI) expressed as the difference between the southeastern and western tropical Indian Ocean SST anomalies (Saji & Vinayachandran, 1999). Weekly DMI data were obtained from the Bureau of Meteorology, Australia [Climate monitoring graphs (bom.gov.au)], and interpolated into a daily time scale.

All data were randomly divided into a training and testing (hold-out) dataset that contained 75% and 25% of the data, respectively, using the sample.split() function of the 'caTools' R package (Tuszynski, 2022). The BRT models were initially fitted to the training dataset with Gaussian distribution using the gbm.step() function of the dismo R package (Elith et al., 2008). The function requires the configuration of parameters including tree complexity (*tc*) that specifies the number of interactions between predictor variables; learning rate (*lr*), which facilitates the contribution of each tree to the growing model; bag fraction (*bf*) that regulates stochasticity by randomly selecting without replacement a specified proportion of the data at each iteration; and step size (*ss*), which controls the number of trees added at each iteration (Elith et al., 2008). The optimal values were identified by testing multiple parameter combinations ($tc = 1–5$, $lr = 0.01, 0.005, 0.001$, $bf = 0.5, 0.7, 0.9$ and $ss = 25$ and 50), resulting in 90 models (Table S1).

Model performance was assessed by testing their ability to predict the number of daily number of detections per tagged *M. alfredi* given the daily values of the predictor variables in the hold-out dataset. Predictions were generated using the predict.gbm() function of the 'gbm' R package (Greenwell et al., 2019). Their accuracy was evaluated using Spearman's rank correlation to compare the observed and predicted daily mean number of detections per tagged *M. alfredi* and the root-mean-square error (RMSE). The model with the highest correlation coefficient and lowest RMSE was selected for further interpretation via partial dependency and interaction plots. The final model was fitted with $tc = 5$, $lr = 0.01$, $bf = 0.5$ and ss = 25 (Table S1).

Partial dependency plots represent the effect of a predictor variable after accounting for the mean effects of all other variables (Hastie et al., 2009). These were generated with confidence intervals (95%) obtained from 1000 bootstrap replicates (Jouffray et al., 2019) and plotted with the ggPD_boot() function of the 'ggBRT' R Package (Jouffray, 2019). For interaction plots, the residual variation between paired model predictions with and without interactions was used to quantify the relative interaction strengths between predictor variables while maintaining the respective means of all other variables (Elith et al., 2008). To determine whether the interactions were significant, 100 bootstrap resampling was performed using the ggInteract_boot() function of the ggBRT R package (Jouffray, 2019), which randomly sampled the daily mean number of *M. alfredi* detections at Egmont Atoll before re-fitting the BRT models. A distribution under the null hypothesis of no interaction among predictors was then generated based on the size of the interaction recorded (Jouffray et al., 2019). The pseudo-determination coefficient percentage of deviance explained (D^2) by the final model was calculated using the following formula (Nieto & Mélin, 2017).

$$D^2 = 1 - (\text{Residual deviance}/\text{Total deviance})$$

3 | RESULTS

3.1 | Season classification

Based on the highest percentage of days each month that the wind direction was predominantly south-easterly (SE monsoon; 101.3°–168.8°) and north-westerly (NW monsoon; 281.3°–348.8°), December to March was classified as the NW monsoon and April to November as the SE monsoon (Figure 2), although April and November are consistent with transitional months between the monsoons.

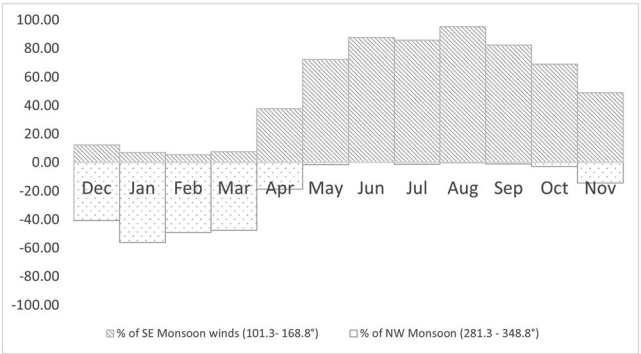

FIGURE 2 Mean monthly wind direction percentage (2010–2020) using south-easterly (SE monsoon; 101.3°–168.8°) and north-westerly (NW monsoon; 281.3°–348.8°). Northwest monsoon wind percentage is transformed ($\chi^* - 1$) to clearly show the monthly variations.

3.2 | Detection summary and residency

For all the 42 tags deployed, there were a total of 205,856 detections between November 2019 and March 2022 (Table 1). The mean (±*SD*) duration between tag deployment and the last detection as of the most recent data download in March 2022 was 257 ± 204 days (range, 2–844).

Excluding tags with track lengths <7 days, the maximum number of consecutive days that each *M. alfredi* was detected on the array ranged from 8 to 319 days (mean = 87 ± 73 days), with the maximum number of days being an adult male (Manta ID: CG-MA-0163). The majority of *M. alfredi* (72%, $n = 29$) had multiple (>3) absences from the array, but extended absences (>2 months) were limited to only seven individuals. Tagged individuals had between 0 and 96 (mean = 15 ± 18 days) absences from the array lasting >1 day. The maximum number of consecutive days that each manta was absent was 0–543 days (mean 39 ± 96 days), with the longest duration being a juvenile female (Manta ID: CG-MA-0128).

Residency indices (Table 1, excluding tags with track lengths <7 days) show that individuals were detected on the Egmont Atoll array for a mean of 77.2 ± 26.1% of the days they were tracked (I_R range 10–100%), with 45% ($n = 18$) of individuals being detected on the array for >90% of their tracking days. Adults and juveniles had similar mean I_R (78.3 ± 28.2% and 76.3 ± 25.3%, respectively). Adult females had the highest mean I_R (83.2 ± 25.9%, $n = 9$), and adult males had the lowest (72.1 ± 31.8%, $n = 7$).

A total of 28,198 resident events (i.e., two or more consecutive detections within 60 min at a single receiver) were identified for the 42 *M. alfredi* between November 2019 and March 2022. Overall, the longest resident event occurred at Manta Alley, lasting 586 mins (Table 2) by a juvenile male (CG-MA-0080). The overall daily mean resident event duration per tagged *M. alfredi* at Egmont Atoll ranged from <10 to 234 min. By location (Figure 3 and Table 2), the maximum daily mean duration occurred at Manta Alley (30 ± 51 min, $n = 2922$ events) and minimum at Ile Tattamucca North (13 ± 25 min, $n = 1686$ events).

3.3 | Demographic, annual and seasonal variations

3.3.1 | Whole of Egmont Atoll

Combining all sites that were monitored throughout Periods 2 and 3 (Period 1 was excluded as only five acoustic receivers were active for 4 months), the daily mean number of detections in Period 2 (21.7 ± 11.5) was significantly higher than in Period 3 (8.3 ± 6.3) as was the daily mean resident duration per tagged *M. alfredi*: Period 2 = 62 ± 36.6 and Period 3 = 27 ± 25.3 (Welch's ANOVA, $F_{1,630} = 394.4$, $p < 0.01$ and $F_{1,700} = 230.9$, $p < 0.01$, respectively; Figure 4).

Including all sites, the daily mean number of detections in the SE monsoon (17 ± 12.1) was significantly higher than the NE monsoon

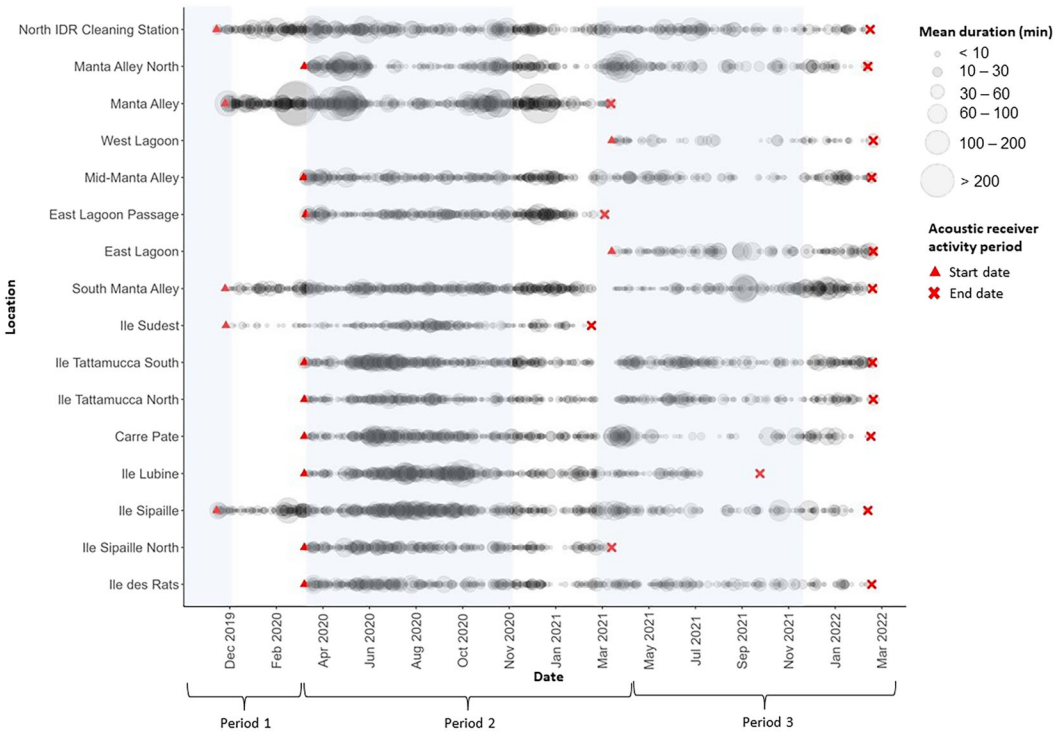

FIGURE 3 Overall mean resident event duration (mins) per tagged *Mobula alfredi* at each location indicated by point size and acoustic receiver deployment date and retrieval date, shown with a red triangle and red cross, respectively. Blue shading and no shading highlight the SE and NW monsoon, respectively. The three Periods in which the data were divided for analysis are indicated at the bottom of the plot (Period 1 = 19 November 2019 to 10 March 2020, Period 2 = 11 March 2020 to 11 April 2021 and Period 3 = 12 April 2021 to 14 March 2022).

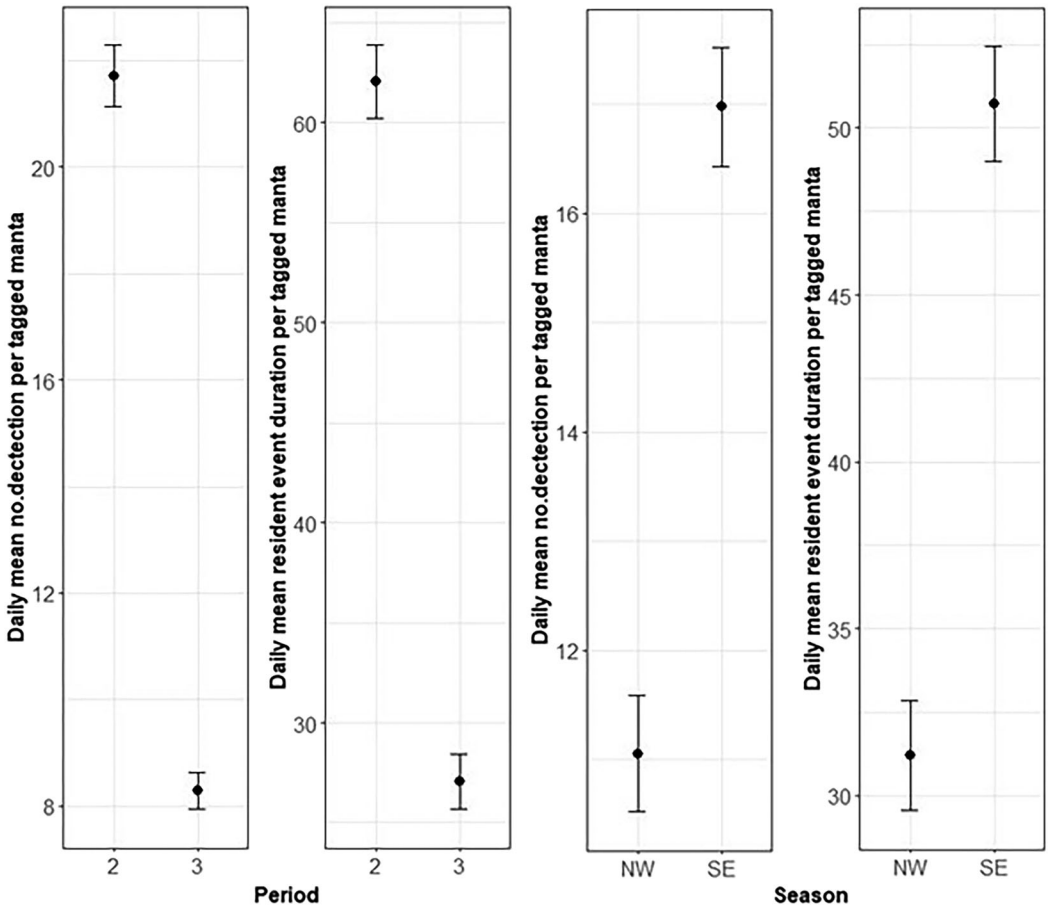

FIGURE 4 Comparison of the daily mean number of detections per tagged *Mobula alfredi* and daily mean resident event duration (mins) between Periods 2 (11 March 2020 to 11 April 2021) and 3 (12 April 2021 to 14 March 2022) including only the detections recorded by acoustic receivers that were continuously active during both periods ($n = 9$, Table 2) and comparison of the daily mean number of detections per tagged *M. alfredi* and daily mean resident event duration (min) between seasons identified in the current study (NW monsoon = December to March and SE monsoon = April to November, Figure 2) for all locations (±se) calculated using only detections that occurred when each location had an active acoustic receiver (Table 2).

(11 ± 9.9) as was the daily mean resident duration per tagged *M. alfredi*: SE monsoon = 50.7 ± 38.5 and NE monsoon = 31.2 ± 30.1 (Welch's ANOVA, $F_{1,818} = 60.4$, $p < 0.01$ and $F_{1,825} = 66.4$, $p < 0.01$, respectively; Figure 4).

3.3.2 | Individual locations at Egmont Atoll

Seasonal variations in visitation patterns and resident events were compared for all locations. There was a significant difference in the daily mean number of tag detections between the NW and SE monsoon at 12 of the 16 locations (Figure 5 and Table S2). Nine of these locations had a significantly higher number during the SE monsoon (Manta Alley North, Ile Sudest, Ile Tattamucca South, Ile Tattamucca North, Carre Pate, Ile Lubine, Ile Sipaille, Ile Sipaille North and Ile des Rats). Apart from Manta Alley North and Ile Sudest, all these locations are situated on the SW face of the atoll. Three locations were higher in the NW monsoon (Mid-Manta Alley, East Lagoon Passage and South Manta Alley), all of which are on the NE face of the atoll. There was no significant difference between seasons at North IdR Cleaning Station, Manta Alley, West Lagoon or East Lagoon.

Daily mean resident event duration per tagged *M. alfredi* was significantly different between the NW and SE monsoon at 12 of the 16 locations (Figure 5 and Table S2), with longer resident events at nine of these locations during the SE monsoon (Manta Alley North, Ile Sudest, Ile Tattamucca South, Ile Tattamucca North, Carre Pate, Ile Lubine, Ile Sipaille, Ile Sipaille North and Ile des Rats). Daily mean resident event duration at Mid-Manta Alley, East Lagoon Passage and South Manta Alley on the NE face of the atoll was significantly longer during the NW monsoon, while there was no significant difference between seasons at four locations (North IdR Cleaning Station, Manta Alley, West Lagoon and East Lagoon).

Resident events were compared by sex and maturity for all locations. Females had significantly longer daily mean resident event durations than males at five of the 16 locations (North IdR Cleaning Station, Mid-Manta Alley, East Lagoon Passage, East Lagoon and Ile Lubine; Figure 6 and Table S3), while males had significantly longer

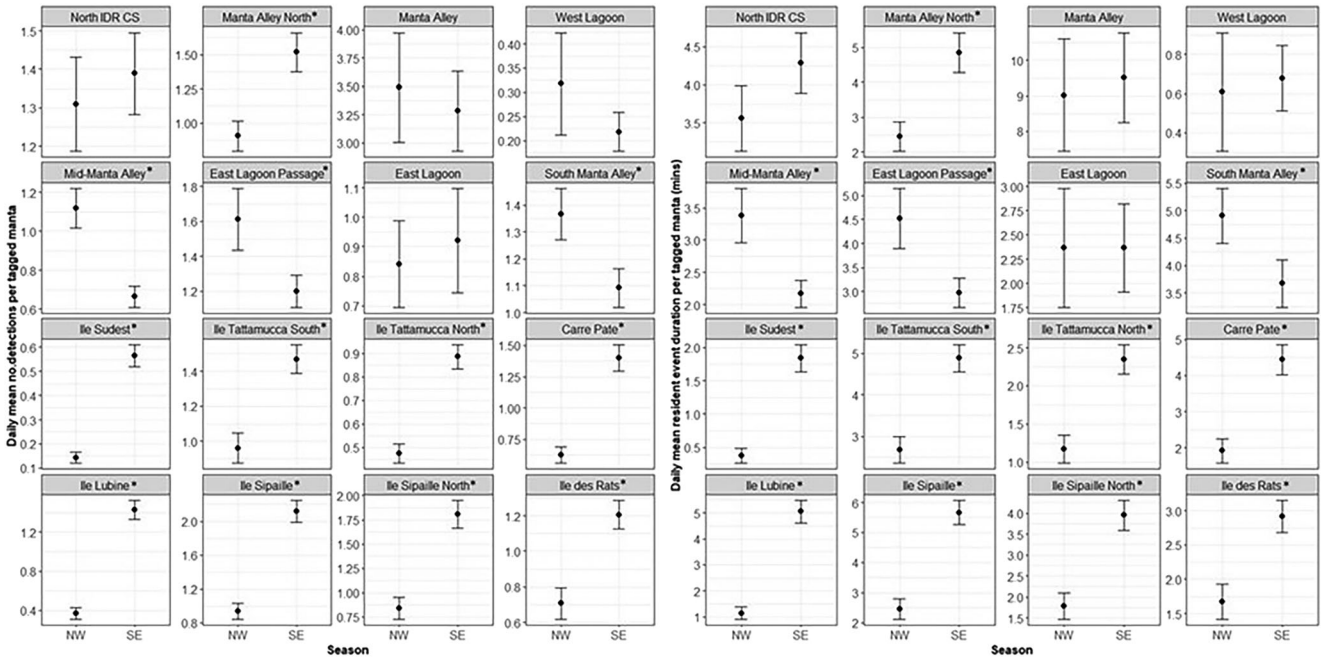

FIGURE 5 Comparison of the daily mean number of *Mobula alfredi* tag detections and daily mean resident event duration (mins) per tagged *M. alfredi* between the seasons identified in the current study (NW monsoon = December to March and SE monsoon = April to November, Figures 1 and 2) for all locations (±se) calculated using detections that occurred when each location had an active acoustic receiver (Table 2). Table 2 depicts the number of days in each season that acoustic receivers were active. An asterisk after the location name indicates there was a significant difference between seasons (Welch's ANOVA, $p < 0.05$; Table S2).

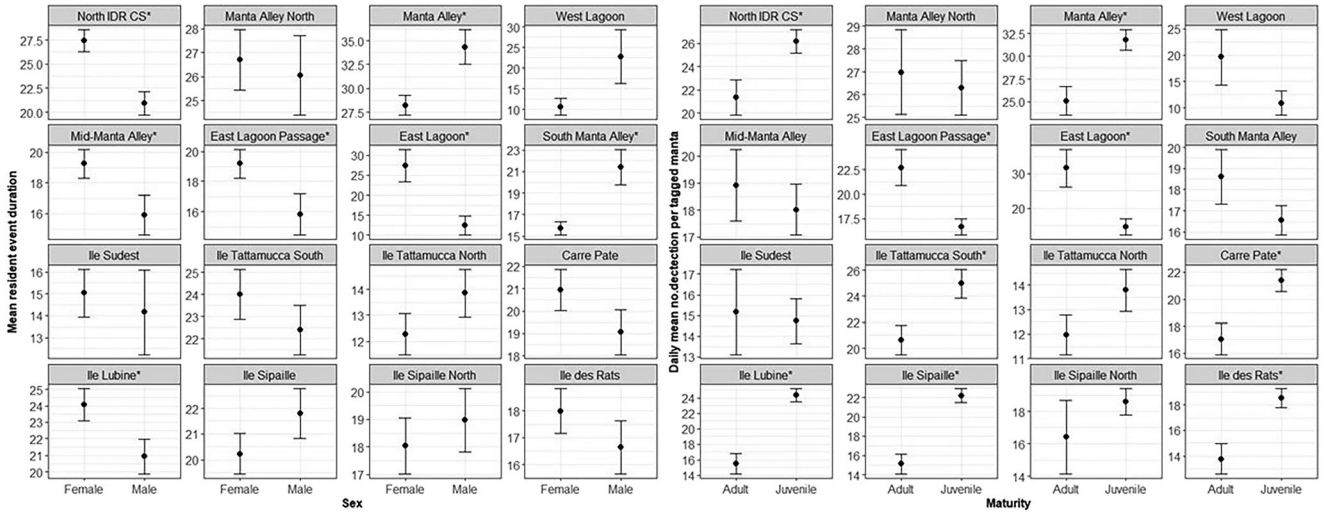

FIGURE 6 Comparison of the overall mean resident event duration by sex and maturity. An asterisk after the location name indicates a significant difference between males and females or adults and juveniles (Welch's ANOVA, $p < 0.05$; Table S3).

durations at Manta Alley and South Manta Alley. There was no significant difference between sexes at eight of the 16 locations (Manta Alley North, West Lagoon, Ile Sudest, Ile Tattamucca South, Ile Tattamucca North, Carre Pate, Ile Sipaillie, Ile Sipaillie North and Ile des Rats). Adults had significantly longer daily mean resident event durations than juveniles at East Lagoon Passage and East Lagoon Figure 6 and Table S3), while juveniles had significantly longer daily mean resident event durations at six of the 16 locations (Manta Alley, Ile Tattamucca South, Carre Pate, Ile Lubine, Ile Sipaillie and Ile des Rats). There was no significant difference in daily mean resident event durations between adults and juveniles at seven of the 16 locations (Manta Alley North, West Lagoon, Mid-Manta Alley, South Manta Alley, Ile Sudest, Ile Tattamucca North or Ile Sipaille North).

3.4 | Boosted regression trees

The final BRT model (Table S1) demonstrated good predictive performance of the daily detections per tagged *M. alfredi* given the daily values of the predictor variables of the hold-out dataset; there was a significant correlation between the actual and predicted data ($r = 0.72$, $p < 0.001$, $n = 92$) and an RMSE of 6.9 daily detections per tagged *M. alfredi* corresponding to 34% of the mean number of observations (range 9–288%). The estimated D^2 suggests that 74% of the deviance was explained by the model.

Partial dependency plots (Figure 7) indicate that the probability of a higher number of detections per tagged *M. alfredi* at Egmont Atoll increased when the DMI showed the IOD was in a positive phase (DMI, 36.9%), with a greater (>25 m) MLD (17.6%). Probability was higher when 50 m depth mean current direction (current direction, 17.5%) was S to SSW (approximately 180–190°), during a new moon (moon phase, 9.9%), with 50 m depth mean temperature <27.5°C (temperature, 9.9%), and with 50 m depth mean current speeds <0.1 ms^{-1} (current speed, 8.3%).

Significant pairwise interactions ($p < 0.01$) occurred between current direction and DMI (Figure 8a), moon phase and DMI (Figure 8b) and MLD and DMI (Figure 8c). These interactions may occur separately or concurrently and may be influenced by other factors; therefore, they should not be considered in isolation (Harris et al., 2021). However, they provide insight into the estimated influence of interrelated processes that can increase the daily mean number of detections per tagged *M. alfredi* at Egmont Atoll. For example, a higher daily mean number of tag detection occurred with S to SSW current directions when the DMI indicated the IOD was in a positive phase (Figure 8a) and with a moon phase of approximately 0.5 (50% illuminated) when the DMI indicated the IOD was in a positive phase (Figure 8b). The interaction between MLD and DMI indicates that a higher daily mean number of tag detection occurred when the MLD was approximately 20 m, and the DMI indicated the IOD was in a positive phase (Figure 8c).

4 | DISCUSSION

The Chagos Archipelago's no-take MPA supports many threatened elasmobranchs [approx. 36 species (Dunn et al., 2022; Harris et al., in review; Stevens, Fernando, et al., 2018; Winterbottom & Anderson, 1997)] for which the current threat of IUU and any future changes to the management of the MPA need to take into account.

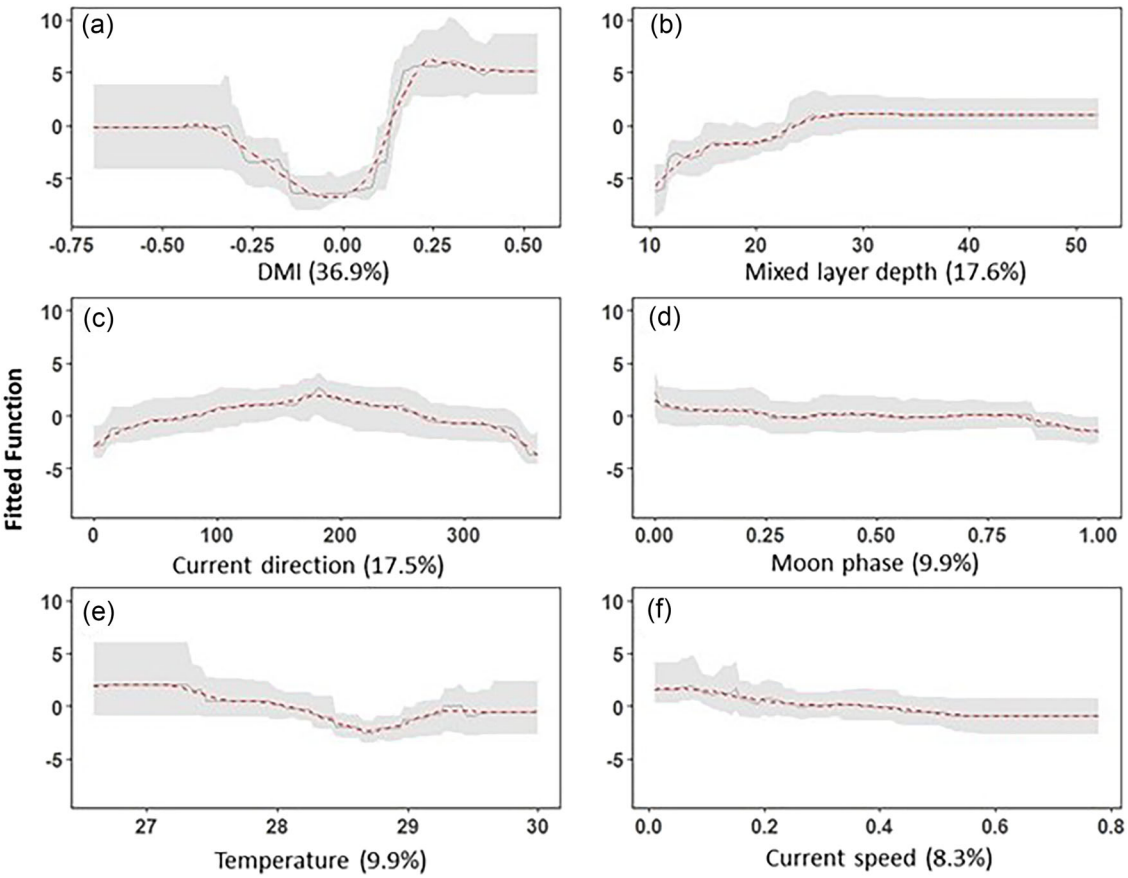

FIGURE 7 Partial dependency plots showing the effect of each predictor variable: (a) dipole mode index (DMI), (b) 50 m depth mean temperature (°C), (c) current direction (°N), (d) moon phase (% illuminated), (e) mixed layer depth (m), (f) current speed (ms^{-1}) on the occurrence of tagged *M. alfredi* at Egmont Atoll while keeping all other variables at their mean. The red dashed line shows smoothed partial decency.

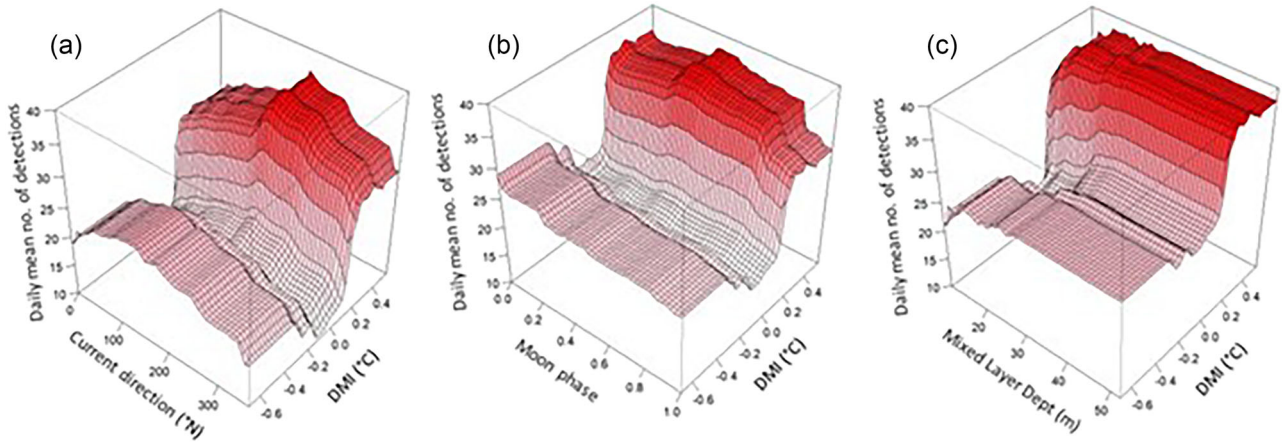

FIGURE 8 Pairwise interactions between predictor variables while keeping all other variables at their respective mean showing the estimated daily mean number of *Mobula alfredi* tag detections at Egmont Atoll; white to red colour gradient indicates lowest to highest. All interactions were significant ($p < 0.01$).

One such species is *M. alfredi*, which aggregates in large numbers at Egmont Atoll (Harris et al., 2021). The current study provides the first insight into how this species utilizes this meso-scale habitat, which hopefully will inform current enforcement patrols and assist future spatial management that will also help to protect many co-occurring elasmobranchs and other marine life.

Overall, *M. alfredi* residency at Egmont Atoll, measured by the residency indices (I_R) of *M. alfredi* with track lengths ≥7 days ($n = 40$), was high (mean $I_R = 77\%$), with 43% of these individuals spending >90% of their tracking days within the range of the acoustic array with extended absences limited to only a few individuals. Similar residency patterns were displayed by adults and juveniles, which supports previous observations at Egmont Atoll, indicating that the location is an important habitat for all life stages (Harris et al., 2021). While it is challenging to compare the level of activity observed between meso-habitats in different regions due to differences in spatial and temporal scales of the acoustic arrays and the number of tagged *M. alfredi* (Appert et al., 2023), it appears that Egmont Atoll has one of the highest levels of *M. alfredi* residency ever observed. For example, compared to studies using the same method of quantifying residency it is substantially higher than Komodo Marine Park, Indonesia (mean $I_R = 29\%$; Dewar et al., 2008), Baa and Lhaviyani Atolls in the Maldives (mean $I_R = 29\%$; Harris & Stevens, 2021), Lady Elliot Island on the Great Barrier Reef [15.3%; residency calculated using a similar method (residency index; RI = number of days detected/Number of days between first and last detection × 100; Couturier et al., 2018)] and the Inhambane Province of Mozambique (mean RI = 15%; Venables et al., 2020). It is also higher than the D'Arros Island and St. Joseph Atoll in Seychelles (mean RI = 62%; Peel et al., 2019).

Regional variations in residency have previously been suggested to be associated with the seasonality of the study location, with higher I_R (RI) occurring at locations where it is absent or limited (Harris & Stevens, 2021). While overall, there was more activity at Egmont Atoll during the SE monsoon, *M. alfredi* were detected in all months of the year throughout the study period. These findings are similar to observations in the Seychelles, where RI (I_R) was high relative to other regions and seasonality was limited (Peel et al., 2019). However, seasonality was also found to be limited in regions where residency was relatively low, such as Komodo Marine Park and Lady Elliot Island (Couturier et al., 2011; Couturier et al., 2018; Dewar et al., 2008). Instead, lower RI may be attributed to acoustic array design (Harris & Stevens, 2021; Peel et al., 2019), which is consistent with the increase in I_R (RI) here compared to that previously observed in a three-and-a-half month (November–March) acoustic tag study at Egmont Atoll (RI = 52%; Harris et al., 2021), when only five acoustic receivers were in place. As well as the increased spatial coverage of the array at Egmont Atoll, the seasonality of the five locations monitored during the earlier study were found here to have either no seasonality or were predominantly utilized during the NW monsoon, while in the current study, nine of the 16 locations monitored were utilized predominantly during the SE monsoon.

By site, all locations on the SW face were predominantly utilized during the SE monsoon, while during the NW monsoon, peaks in activity occur on the NE face, which is similar to the seasonal use of different sides of the atoll (east and west) in the Maldives (Harris et al., 2020). However, four locations on the NE face exhibited no seasonality, which includes Manta Alley, a feeding aggregation site that has been shown to provide temporally limited prey resources influenced by the site's geomorphology, and fine-scale oceanographic processes, including the tide, near-seabed temperature and upwelling/downwelling (Harris et al., 2021; Robinson et al., 2023). North IdR Cleaning Station was also found to be nonseasonal, which is consistent with it being located close to the nonseasonal feeding site, Manta Alley, as *M. alfredi* will typically frequent cleaning stations that are close to feeding areas (Armstrong et al., 2021; Harris et al., 2020; Stevens, 2016; Stevens, Hawkins & Roberts, 2018).

The intensity, measured by resident event duration, at which *M. alfredi* utilizes different sites around the atoll varied between demographics. Juveniles spent more time on the SW face of the atoll,

while adults more intensively utilized the passageway at East Lagoon Passage and East Lagoon. This passageway is one of the narrowest observed along the Egmont Atoll's northeast rim and experiences extremely strong currents (P. Hosegood and E. Robinson, unpublished data) that likely transport zooplankton into the lagoon from the thermocline, leading to peaks in prey biomass similar to Manta Alley (Harris et al., 2021). However, water entering (or exiting) the lagoon may become much more restricted than those flowing in at Manta Alley, potentially leading to intense jet-like flows that may make it less energetically efficient for juveniles forage due to the increased hydrodynamical drag with smaller body size (Nøttestad et al., 1999).

There was a significant decline in the daily mean number of detections and daily mean resident event duration per tagged *M. alfredi* between Period 2 (March 2020–April 2021) and Period 3 (April 2021–March 2022). While this decline could be associated with the exclusion of some sites from the analysis, for example, the most active, non-seasonal location, Manta Alley, they also coincide with a 19-fold increase in number of IUU fishing vessels that occurred in the Chagos Archipelago (Collins et al., 2023). Manta rays have been seized from illegal fishers by enforcement authorities in the region's MPA (Collins, Nuno, Broderick, et al., 2021), so this decline is of particular concern and further research is required to assess the extent of this potential threat. However, the decline could be associated with changes in environmental conditions that may have reduced prey resources (Harris et al., 2021). Here, an assessment of the environmental influences of *M. alfredi* activity at Egmont Atoll via BRT modelling highlighted various processes that appear to be associated with an increase in the probability of detections. For example, a high probability occurred when the IOD was in a positive phase and with a greater MLD, which supports *in situ* observation of higher productivity at Egmont Atoll under these conditions (Robinson et al., 2023). These two variables also showed a significant interaction effect whereby a positive IOD and deeper mixed layer increased the probability of detections, which reflects the characteristic deepening of the thermocline during a positive IOD phase (Du et al., 2020; Lee et al., 2022; Ratna et al., 2021; Robinson et al., 2023; Shi & Wang, 2021). The strongest positive IOD event of the 21st century occurred in 2019, the effects of which led to a depression of chl-α levels in the Indian Ocean that persisted until mid-2020 (Shi & Wang, 2021). During this time, *M. alfredi* potentially relied more heavily on the enhanced levels of prey associated with localized oceanographic processes at Egmont Atoll (Harris et al., 2021; Harris et al., 2023; Robinson et al., 2023), which could have led to the decline in activity that occurred between 2020 and 2021 when reliance on the location may have reduced with an increase in prey resources elsewhere.

The BRT model also suggests that an increased presence of *M. alfredi* at Egmont Atoll was associated with ocean currents flowing S to SSW. Winds influence the flow of ocean surface currents that can lead to enhanced productivity on the leeward side of an atoll through deep-water upwellings that carry nutrient-rich water into the euphotic zone (Deik et al., 2017; Doty & Oguri, 1956; Sasamal, 2006). In the Maldives, this process is linked to the biannual reversal of winds and the seasonal east–west and west–east migration pattern of *M. alfredi* (Anderson et al., 2011; Harris et al., 2020). Here, a higher level of activity occurred on the SW face of the atoll during SE monsoon when winds are likely to be driving ocean surface currents SW, thus potentially enhancing productivity and prey availability on this side of the atoll.

Mobula alfredi presence was also influenced by moon phase, which has been associated with *M. alfredi* presence at other meso-scale habitats, such as in the Maldives, where three acoustically monitored sites were all frequented during different moon phases, which was suggested to be associated with the lunar effect on tidal intensity (Harris & Stevens, 2021). Tidal dynamics have previously been shown to influence visitation patterns at Manta Alley; for example, during a flood tide, zooplankton may be transported from the thermocline with cold-water bores that propagate up the atoll slope and into the lagoon (Harris et al., 2021; Robinson et al., 2023), which is consistent with the higher probability of detections with lower SST observed here. Greater tidal intensity potentially enhances this and other localized processes that increase prey availability around Egmont Atoll. However, *M. alfredi* activity appears to decline with increased current speeds and between a new and full moon; therefore, the lunar effects may be associated with their influence on the extent of vertical movement of zooplankton. During times of high moon illumination, zooplankton moves deeper within the water column, potentially leading to *M. alfredi* foraging away from shallow coastal locations as moon illumination increases (Braun et al., 2014; Couturier et al., 2018; Peel et al., 2019). This pattern has been observed in the Chagos Archipelago and meso-scale habitats, such as at D'Arros Island, Seychelles and at Lady Elliot Island, Australia (Andrzejaczek et al., 2020; Couturier et al., 2018; Peel et al., 2019), where similar to the current study, acoustic receivers were located in shallow coastal reef habitats (Andrzejaczek et al., 2020; Couturier et al., 2018; Peel et al., 2019). In contrast, the interaction effect between the moon phase and the IOD suggests that moon illumination might be less influential when the IOD is in a strong positive phase with a high number of detections estimated to occur throughout the lunar cycle.

4.1 | Conservation concerns and recommendations

The frequency at which Egmont Atoll is utilized by *M. alfredi* highlights that the location is a crucial year-round habitat for the region's population, where the species are particularly vulnerable to anthropogenic disturbance. The immediate concern is the recent increase in IUU fishing activity (Collins et al., 2023), from which *M. alfredi* are most likely to be at risk when utilizing the shallow coastal areas of the atoll. Regular enforcement patrols are recommended, with prioritization between April to November (SE monsoon), particularly during a new moon.

With bilateral negotiations underway between the UK and Mauritius governments, any changes in sovereignty and the current MPA should recognize the importance of this location and ensure the protection of manta rays. Protection measures should include

the listing of *M. alfredi* as a nationally protected species in Mauritius. It is recommended that any future spatial planning of the MPA should ensure that strict no-take regulations remain in place around Egmont Atoll with active on-site enforcement. Additionally, speed restrictions should be imposed for all vessels to minimize the risk posed by increased boat traffic (Strike et al., 2022). Similar to other regions, the shallow coastal environment at Egmont Atoll provides essential resources to many cooccurring species, in particular, other vulnerable elasmobranch species that share the same conservative life history traits as *M. alfredi* (Dulvy, Fowler, et al., 2014; Harris et al., 2020; O'Shea et al., 2010; Rohner et al., 2017; Stewart et al., 2017). Therefore, prioritizing current enforcement patrols and ensuring Egmont Atoll is adequately protected in the future will serve to protect a multitude of species, as well as habitats, the results of which will propagate throughout the entire marine ecosystem (Harris et al., 2020). It is also essential that the scientific research that has been conducted at Egmont Atoll and other areas throughout the archipelago continues. For example, satellite telemetry studies should be used to identify other key habitats and understand the wider movement of *M. alfredi*, as this provides the foundation for developing effective conservation management strategies.

ACKNOWLEDGEMENTS

We express our sincerest gratitude to the Bertarelli Foundation and the Garfield Weston Foundation, whose generous support made this research possible. This study contributes to the Bertarelli Programme in Marine Science. We thank the British Indian Ocean Territory Administration (BIOTA) for granting us permission to undertake the research. Thank you to the Manta Trust team and everyone else who assisted in the field and beyond: Rebecca Carter, Simon Hilbourne and Annie Murray, Rhys Diplock, Claire Collins, Anna Patal, Marleen Stuhr, Craig and Mickael and all the research vessel crew. Thank you to the two anonymous reviewers for offering constructive feedback, which improved the manuscript.

CONFLICT OF INTEREST STATEMENT

The authors declare that they have no known competing financial interests or personal relationships that could have appeared to influence the work reported in this paper.

DATA AVAILABILITY STATEMENT

The data that support the findings of this study are available from the corresponding author upon reasonable request.

ORCID

Joanna L. Harris https://orcid.org/0000-0001-8684-9096
Guy M. W. Stevens https://orcid.org/0000-0002-2056-9830

REFERENCES

Afonso, P., Fontes, J., Holland, K.N. & Santos, R.S. (2008) Social status determines behaviour and habitat usage in a temperate parrotfish: implications for marine reserve design. *Marine Ecology Progress Series*, 359, 215–227. https://doi.org/10.3354/meps07272

Anderson, R.C., Adam, M.S. & Goes, J.I. (2011) From monsoons to mantas: seasonal distribution of *Manta alfredi* in the Maldives. *Fisheries Oceanography*, 20(2), 104–113. https://doi.org/10.1111/j.1365-2419.2011.00571.x

Andrzejaczek, S., Chapple, T.K., Curnick, D.J., Carlisle, A.B., Castleton, M., Jacoby, D.M.P. et al. (2020) Individual variation in residency and regional movements of reef manta rays *Mobula alfredi* in a large marine protected area. *Marine Ecology Progress Series*, 639, 137–153. https://doi.org/10.3354/meps13270

Appert, C., Udyawer, V., Simpfendorfer, C., Heupel, M., Scott, M., Currey-Randall, L. et al. (2023) Use, misuse, and ambiguity of indices of residence in acoustic telemetry studies. *Marine Ecology Progress Series*, 714, 27–44. https://doi.org/10.3354/meps14300

Armstrong, A.O., Armstrong, A.J., Bennett, M.B., Richardson, A.J., Townsend, K.A., Everett, J.D. et al. (2021) Mutualism promotes site selection in a large marine planktivore. *Ecology and Evolution*, 11(10), 5606–5623. https://doi.org/10.1002/ece3.7464

Bovalo, C. & Barthe, C. (2012) System sciences a lightning climatology of the South-West Indian Ocean. *Natural Hazards and Earth System Sciences*, 12, 2659–2670. https://doi.org/10.5194/nhess-12-2659-2012

Braun, C.D., Skomal, G.B., Thorrold, S.R. & Berumen, M.L. (2014) Diving behavior of the reef manta ray links coral reefs with adjacent deep pelagic habitats. *PLoS ONE*, 9(2), e88170. https://doi.org/10.1371/journal.pone.0088170

Campbell, H.A., Watts, M.E., Dwyer, R.G. & Franklin, C.E. (2012) V-track: software for analysing and visualising animal movement from acoustic telemetry detections. *Marine and Freshwater Research*, 63(9), 815–820. https://doi.org/10.1071/MF12194

Carlisle, A.B., Tickler, D., Dale, J.J., Ferretti, F., Curnick, D.J., Chapple, T.K. et al. (2019) Estimating space use of mobile fishes in a large marine protected area with methodological considerations in acoustic Array design. *Frontiers in Marine Science*, 6, 256. https://doi.org/10.3389/fmars.2019.00256

Carpenter, M., Parker, D., Dicken, M.L. & Grif, C.L. (2023) Multi-decade catches of manta rays (*Mobula alfredi*, *M. birostris*) from South Africa reveal significant decline. *Frontiers in Marine Science*, 10, 1128819. https://doi.org/10.3389/fmars.2023.1128819

Clark, MJ., Duffy, H., Pearce, J., Mees, C., (2015). Update on the catch and bycatch composition of illegal fishing in the British Indian Ocean Territory (BIOT) and a summary of abandoned and lost fishing, IOTC Working Party on Ecosystem and Bycatch (WPEB) WPEB11–48.

Collins, C., Kerry, C., de Vos, A., Karnad, D., Nuno, A. & Letessier, T.B. (2023) Changes in illegal fishing dynamics in a large-scale MPA during COVID-19. *Current Biology*, 33(16), R851–R852. https://doi.org/10.1016/j.cub.2023.05.076

Collins, C., Nuno, A., Benaragama, A., Broderick, A., Wijesundara, I., Wijetunge, D. et al. (2021) Ocean-scale footprint of a highly mobile fishing fleet: social-ecological drivers of fleet behaviour and evidence of illegal fishing. *People and Nature*, 3(3), 740–755. https://doi.org/10.1002/pan3.10213

Collins, C., Nuno, A., Broderick, A., Curnick, D.J., de Vos, A., Franklin, T. et al. (2021) Understanding persistent non-compliance in a remote, large-scale marine protected area. *Frontiers in Marine Science*, 8,, 650276. https://doi.org/10.3389/fmars.2021.650276

Couturier, L.I.E., Jaine, F.R.A., Townsend, K.A., Weeks, S.J., Richardson, A.J. & Bennett, M.B. (2011) Distribution, site affinity and regional movements of the manta ray, *Manta alfredi* (Krefft, 1868), along the east coast of Australia. *Marine and Freshwater Research*, 62, 628–637. https://doi.org/10.1071/MF10148

Couturier, L.I.E., Marshall, A.D., Jaine, F.R.A., Kashiwagi, T., Pierce, S.J., Townsend, K.A. et al. (2012) Biology, ecology and conservation of the Mobulidae. *Journal of Fish Biology*, 80, 1075–1119. https://doi.org/10.1111/j.1095-8649.2012.03264.x

Couturier, L.I.E., Newman, P., Jaine, F.R.A., Bennett, M.B., Venables, W.N., Cagua, E.F. et al. (2018) Variation in occupancy and habitat use of *Mobula alfredi* at a major aggregation site. *Marine Ecology Progress Series*, 599, 125–145. https://doi.org/10.3354/meps12610

Crowder, L.B., Hazen, E.L., Avissar, N., Bjorkland, R., Latanich, C. & Ogburn, M.B. (2008) The impacts of fisheries on marine ecosystems and the transition to ecosystem-based management. *Annual Review of Ecology, Evolution, and Systematics*, 39, 259–278. https://doi.org/10.1146/annurev.ecolsys.39.110707.173406

Curnick, D.J., Feary, D.A. & Cavalcante, G.H. (2021) Risks to large marine protected areas posed by drifting fish aggregation devices. *Conservation Biology*, 35(4), 1222–1232. https://doi.org/10.1111/cobi.13684

Deik, H., Reuning, L. & Pfeiffer, M. (2017) Orbital scale variation of primary productivity in the central equatorial Indian Ocean (Maldives) during the early Pliocene. *Palaeogeography Palaeoclimatology Palaeoecology*, 480, 33–41. https://doi.org/10.1016/j.palaeo.2017.05.012

Derville, S., Constantine, R., Baker, C., Oremus, M. & Torres, L. (2016) Environmental correlates of nearshore habitat distribution by the critically endangered Maüi dolphin. *Marine Ecology Progress Series*, 551, 261–275. https://doi.org/10.3354/meps11736

Dewar, H., Mous, P., Domeier, M., Muljadi, A., Pet, J. & Whitty, J. (2008) Movements and site fidelity of the giant manta ray, Manta birostris, in the Komodo Marine Park, Indonesia. *Marine Biology*, 155(2), 121–133. https://doi.org/10.1007/s00227-008-0988-x

Doty, M. & Oguri, M.S. (1956) The island mass effect. *ICES Journal of Marine Science*, 22(1), 33–37. https://doi.org/10.1093/icesjms/22.1.33

Du, Y., Zhang, Y., Zhang, L.Y., Tozuka, T., Ng, B. & Cai, W. (2020) Thermocline warming induced extreme Indian Ocean Dipole in 2019. *Geophysical Research Letters*, 47(18), 1–10. https://doi.org/10.1029/2020GL090079

Dulvy, N.K., Fowler, S.L., Musick, J.A., Cavanagh, R.D., Kyne, P.M., Harrison, L.R. et al. (2014) Extinction risk and conservation of the world's sharks and rays. *eLife*, 3, e00590. https://doi.org/10.7554/eLife.00590.001

Dulvy, N.K., Pardo, S.A., Simpfendorfer, C.A. & Carlson, J.K. (2014) Diagnosing the dangerous demography of manta rays using life history theory. *PeerJ*, 2, e400. https://doi.org/10.7717/peerj.400

Dulvy, N.K., Simpfendorfer, C.A., Davidson, L.N.K., Fordham, S.V., Bräutigam, A., Sant, G. et al. (2017) Challenges and priorities in shark and ray conservation. *Current Biology*, 27(11), R565–R572. https://doi.org/10.1016/j.cub.2017.04.038

Dunn, N., Savolainen, V., Weber, S., Andrzejaczek, S., Carbone, C. & Curnick, D. (2022) Elasmobranch diversity across a remote coral reef atoll revealed through environmental DNA metabarcoding. *Zoological Journal of the Linnean Society*, 196(2), 593–607. https://doi.org/10.1093/zoolinnean/zlac014

Elith, J., Leathwick, J.R. & Hastie, T. (2008) A working guide to boosted regression trees. *The Journal of Animal Ecology*, 77(4), 802–813. https://doi.org/10.1111/j.1365-2656.2008.01390.x

Fernando, D. & Stewart, J.D. (2021) High bycatch rates of manta and devil rays in the "small-scale" artisanal fisheries of Sri Lanka. *PeerJ*, 9, e11994. https://doi.org/10.7717/peerj.11994

Ferretti, F., Curnick, D., Liu, K., Romanov, E.V. & Block, B.A. (2018) Shark baselines and the conservation role of remote coral reef ecosystems. *Science Advances*, 4(3). https://doi.org/10.1126/sciadv.aaq0333

Greenwell, B., Boehmke, B., Cunningham, J., 2019. Generalized Boosted Regression Models Package 'gbm'.

Harris, J.L., 2019. Habitat use of reef manta rays, *Mobula alfredi*, in the Chagos archipelago and the effectiveness of the region's marine protected area for this vulnerable species. MRes Thesis. University of Plymouth.

Harris, J.L., Collins, C., Spalding, M. & Stevens, G.M.W. First records of the sicklefin (*Mobula tarapacana*), bentfin (*M. Thurstoni*) and spinetail (*M. Mobular*) devil rays in the Chagos archipelago. *Journal of Fish Biology*. (in review).

Harris, J.L., Embling, C.B., Alexander, G., Curnick, D., Roche, R., Froman, N. et al. (2023) Intraspecific differences in short- and long-term foraging strategies of reef manta ray (*Mobula alfredi*) in the Chagos archipelago. *Global Ecology and Conservation*, 46, e02636. https://doi.org/10.1016/j.gecco.2023.e02636

Harris, J.L., Hosegood, P., Robinson, E., Embling, C.B., Hilbourne, S. & Stevens, G.M.W. (2021) Fine-scale oceanographic drivers of reef manta ray (*Mobula alfredi*) visitation patterns at a feeding aggregation site. *Ecology and Evolution*, 11(9), 4588–4604. https://doi.org/10.1002/ece3.7357

Harris, J.L., Mcgregor, P.K., Oates, Y. & Stevens, G.M.W. (2020) Gone with the wind: seasonal distribution and habitat use by the reef manta ray (Mobula alfredi) in the Maldives, implications for conservation. *Aquatic Conservation: Marine and Freshwater Ecosystems*, 30, 1649–1664. https://doi.org/10.1002/aqc.3350

Harris, J.L. & Stevens, G.M.W. (2021) Environmental drivers of reef manta ray (*Mobula alfredi*) visitation patterns to key aggregation habitats in the Maldives. *PLoS ONE*, 16, e0252470. https://doi.org/10.1371/journal.pone.0252470

Harris, J.L. & Stevens, G.M.W. The illegal exploitation of threatened manta and devil rays in the Chagos archipelago, one of the world's largest no-take MPAs. *Marine Policy*. (in review).

Hastie, T., Tibshirani, R. & Friedman, J. (2009) *The elements of statistical learning the elements of statistical learning data mining, inference, and prediction*, 2nd edition, New York: Springer-Verlag.

Hays, G.C., Koldewey, H.J., Andrzejaczek, S., Attrill, M.J., Barley, S., Bayley, D.T.I. et al. (2020) A review of a decade of lessons from one of the world's largest MPAs: conservation gains and key challenges. *Marine Biology*, 167(11), 1–22. https://doi.org/10.1007/s00227-020-03776-w

Hosegood, J., Humble, E., Ogden, R., de Bruyn, M., Creer, S., Stevens, G.M.W. et al. (2020) Phylogenomics and species delimitation for effective conservation of manta and devil rays. *Molecular Ecology*, 29(24), 4783–4796. https://doi.org/10.1111/mec.15683

Humble, E., Hosegood, J., Carvalho, G., de Bruyn, M., Creer, S., Stevens, M.W., Armstrong, A., Bonfil, R., Deakos, M., Fernando, D., Peel, L.R., Pollett, S., Ponzo, A., Stewart, J.D., Wintner, S., Ogden, R., 2023. Comparative population genomics of manta rays has global implications for management. bioRxiv Prepr. 24. https://doi.org/10.1101/2023.06.19.545572

Jacoby, D.M.P., Ferretti, F., Freeman, R., Carlisle, A.B., Chapple, T.K., Curnick, D.J. et al. (2020) Shark movement strategies influence poaching risk and can guide enforcement decisions in a large, remote marine protected area. *Journal of Applied Ecology*, 57(9), 1782–1792. https://doi.org/10.1111/1365-2664.13654

Jouffray, J.-B. (2019) *ggBRT: explore and visualise the results of boosted regression trees*. R Package.

Jouffray, J.-B., Wedding, L.M., Norstro, A.V., Donovan, M.K., Williams, G.J., Crowder, L.B. et al. (2019) Parsing human and biophysical drivers of coral reef regimes. *Proceedings B*, 268(1896), 20182544. https://doi.org/10.1098/rspb.2018.2544

Kashiwagi, T., Marshall, A.D., Bennett, M.B. & Ovenden, J.R. (2011) Habitat segregation and mosaic sympatry of the two species of manta ray in the Indian and Pacific oceans: *Manta alfredi* and *M. Birostris*. *Marine Biodiversity Records*, 4, e53. https://doi.org/10.1017/S1755267211000881

Lee, E., Kim, C. & Na, H. (2022) Suppressed upwelling events in the Seychelles—Chagos thermocline ridge of the southwestern tropical Indian Ocean. *Ocean Science Journal*, 57(2), 305–313. https://doi.org/10.1007/s12601-022-00075-x

Marshall, A., Barreto, R., Carlson, J., Fernando, D., Fordham, S., Francis, M.P., Herman, K., Jabado, R.W., Liu, K.M., Pacoureau, N., Rigby, C.L., Romanov, E., Sherley, R.B., 2022. *Mobula alfredi* (amended

version of 2019 assessment). IUCN Red List Threat. Species™ ISSN 8235, e.T195459A214395983.

Marshall, A.D., Compagno, L.J.V. & Bennett, M.B. (2009) Redescription of the genus Manta with resurrection of *Manta alfredi* (Krefft, 1868) (Chondrichthyes; Myliobatoidei; Mobulidae). *Zootaxa*, 2301, 1–28. https://doi.org/10.5281/zenodo.191734

Murray, A., Garrud, E., Ender, I., Lee-Brooks, K., Atkins, R., Lynam, R. et al. (2019) Protecting the million-dollar mantas; creating an evidence-based code of conduct for manta ray tourism interactions. *Journal of Ecotourism*, 19(2), 132–147. https://doi.org/10.1080/14724049.2019.1659802

Nieto, K. & Mélin, F. (2017) Variability of chlorophyll-a concentration in the Gulf of Guinea and its relation to physical oceanographic variables. *Progress in Oceanography*, 151, 97–115. https://doi.org/10.1016/j.pocean.2016.11.009

Notarbartolo di Sciara, G., Adnet, S., Bennett, M., Broadhurst, M.K., Fernando, D., Jabado, R.W. et al. (2020) Taxonomic status, biological notes, and conservation of the longhorned pygmy devil ray *Mobula eregoodoo* (cantor, 1849). *Aquatic Conservation: Marine and Freshwater Ecosystems*, 30(1), 104–122. https://doi.org/10.1002/aqc.3230

Nøttestad, L., Giske, J., Holst, J.C. & Huse, G. (1999) A length-based hypothesis for feeding migrations in pelagic fish. *Canadian Journal of Fisheries and Aquatic Sciences*, 56(S1), 26–34. https://doi.org/10.1139/f99-222

O'Shea, O.R., Kingsford, M.J. & Seymour, J. (2010) Tide-related periodicity of manta rays and sharks to cleaning stations on a coral reef. *Marine and Freshwater Research*, 61, 65–73. https://doi.org/10.1071/MF08301

Peel, L.R., Stevens, G., Daly, R., Daly, C., Lea, J., Clarke, C. et al. (2019) Movement and residency patterns of reef manta rays *Mobula alfredi* in the Amirante Islands, Seychelles. *Marine Ecology Progress Series*, 621, 169–184. https://doi.org/10.3354/meps12995

Price, A.R.G., Harris, A., Mcgowan, A., Venkatachalam, A.J., Sheppard, C.R.C. & Campus, C. (2010) Chagos feels the pinch: assessment of holothurian (sea cucumber) abundance, illegal harvesting and conservation prospects in. *British Indian Ocean Territory*, 20(1), 117–126. https://doi.org/10.1002/aqc.1054

R Core Team. 2023. R: a language and environment for statistical computing. R Foundation for Statistical Computing [WWW Document]. URL http://www.r-project.org/

Ratna, S.B., Cherchi, A., Osborn, T.J., Joshi, M. & Uppara, U. (2021) The extreme positive Indian Ocean dipole of 2019 and associated Indian summer monsoon rainfall response. *Geophysical Research Letters*, 48 (2), 1–11. https://doi.org/10.1029/2020GL091497

Robinson, E., Hosegood, P. & Bolton, A. (2023) Dynamical oceanographic processes impact on reef manta ray behaviour: extreme Indian Ocean dipole influence on local internal wave dynamics at a remote tropical atoll. *Progress in Oceanography*, 103129. https://doi.org/10.1016/j.pocean.2023.103129

Rohner, C.A., Flam, A.L., Pierce, S.J. & Marshall, A.D. (2017) Steep declines in sightings of manta rays and devilrays (Mobulidae) in southern Mozambique. *PeerJ Preprints*, 5, e3051v1. https://doi.org/10.7287/peerj.preprints.3051v1

Rohner, C.A., Pierce, S.J., Marshall, A.D., Weeks, S.J., Bennett, M.B. & Richardson, A.J. (2013) Trends in sightings and environmental influences on a coastal aggregation of manta rays and whale sharks. *Marine Ecology Progress Series*, 482, 153–168. https://doi.org/10.3354/meps10290

Saji, N.H. & Vinayachandran, P.N. (1999) A dipole mode in the tropical Indian Ocean. *Nature*, 401, 360–363. https://doi.org/10.1038/43854

Sasamal, S.K. (2006) Island mass effect around the Maldives during the winter months of 2003 and 2004. *International Journal of Remote Sensing*, 27(22), 5087–5093. https://doi.org/10.1080/01431160500177562

Sheppard, C.R., Ateweberhan, M., Bowen, B.W., Carr, P., Chen, C.A., Clubbe, C. et al. (2012) Reefs and islands of the Chagos archipelago, Indian Ocean: why it is the world's largest no-take marine protected area. *Aquatic Conservation: Marine and Freshwater Ecosystems*, 22(2), 232–261. https://doi.org/10.1002/aqc.1248

Sheppard, C.R.C., Seaward, M.R.D., Klaus, R. & Topp, J.M.W. (1999) The Chagos Archipelago: an introduction. In: Sheppard, C.R.C., & Seaward, M.R.D. (Eds.) *Ecology of the Chagos Archipelago*, Otley: Westbury Publishing (Linnean Society Occasional Publications 2).

Shi, W. & Wang, M. (2021) A biological Indian Ocean Dipole event in 2019. *Scientific Reports*, 11(1), 1–8. https://doi.org/10.1038/s41598-021-81410-5

Silber, G.K., Lettrich, M.D., Thomas, P.O., Baker, J.D., Baumgartner, M., Becker, E.A. et al. (2017) Projecting marine mammal distribution in a changing climate. *Frontiers in Marine Science*, 4. https://doi.org/10.3389/fmars.2017.00413

Simpfendorfer, C.A., Huveneers, C., Steckenreuter, A., Tattersall, K., Hoenner, X., Harcourt, R. et al. (2015) Ghosts in the data: false detections in VEMCO pulse position modulation acoustic telemetry monitoring equipment. *Animal Biotelemetry*, 3(55). https://doi.org/10.1186/s40317-015-0094-z

Stevens, G.M.W., 2016. Conservation and population ecology of Manta rays in the Maldives. PhD Thesis. University of York.

Stevens, G.M.W., Fernando, D., Dando, M. & di Sciara, G.N. (2018) *Guide to the manta and devil rays of the world*: Princeton University Press.. https://doi.org/10.2307/j.ctvs32s7t

Stevens, G.M.W. & Froman, N. (2018) The Maldives Archipelago. In: Sheppard, C. (Ed.) *World seas: an environmental evaluation*. Volume II, The Indian Ocean to the Pacific, London: Academic Press, pp. 211–236.

Stevens, G.M.W., Hawkins, J.P. & Roberts, C.M. (2018) Courtship and mating behaviour of manta rays *Mobula alfredi* and *M. Birostris* in the Maldives. *Journal of Fish Biology*, 93(2), 344–359. https://doi.org/10.1111/jfb.13768

Stewart, J.D., Rohner, C.A., Araujo, G., Avila, J., Fernando, D., Forsberg, K. et al. (2017) Trophic overlap in mobulid rays: insights from stable isotope analysis. *Marine Ecology Progress Series*, 580, 131–151. https://doi.org/10.3354/meps12304

Strating, R. (2023) The rules-based order as rhetorical entrapment: comparing maritime dispute resolution in the Indo-Pacific. *Content Security Policy*, 44(3), 372–409. https://doi.org/10.1080/13523260.2023.2204266

Strike, E.M., Harris, J.L., Ballard, K.L., Hawkins, J.P., Crockett, J. & Stevens, G.M.W. (2022) Sublethal injuries and physical abnormalities in Maldives manta rays, *Mobula alfredi* and *Mobula birostris*. *Frontiers in Marine Science*, 9, 773897. https://doi.org/10.3389/fmars.2022.773897

Tickler, D.M., Carlisle, A.B., Chapple, T.K., Curnick, D.J., Dale, J.J., Schallert, R.J. et al. (2019) Potential detection of illegal fishing by passive acoustic telemetry. *Animal Biotelemetry*, 7(1), 1–11. https://doi.org/10.1186/s40317-019-0163-9

Tuszynski, J., 2022. Tools: moving window statistics, GIF, Base64, ROC AUC, etc package 'caTools' [WWW document]. URL https://cran.r-project.org/web/packages/caTools/caTools.pdf

Venables, S.K., van Duinkerken, D.I., Rohner, C.A. & Marshall, A.D. (2020) Habitat use and movement patterns of reef manta rays Mobula alfredi in southern Mozambique. *Marine Ecology Progress Series*, 634, 99–114. https://doi.org/10.3354/meps13178

Venables, S., Mcgregor, F., Brain, L. & Van Keulen, M. (2016) Manta ray tourism management, precautionary strategies for a growing industry: a case study from the Ningaloo Marine Park, Western Australia. *Pacific Conservation Biology*, 22(4), 295–300. https://doi.org/10.1071/PC16003

Ward-Paige, C.A., Davis, B. & Worm, B. (2013) Global population trends and human use patterns of manta and Mobula rays. *PLoS ONE*, 8(9), e74835. https://doi.org/10.1371/journal.pone.0074835

White, W.T., Corrigan, S., Yang, L., Henderson, A.C., Bazinet, A.L., Swofford, D.L. et al. (2017) Phylogeny of the manta and devilrays

(Chondrichthyes: mobulidae), with an updated taxonomic arrangement for the family. *Zoological Journal of the Linnean Society*, 182(1), 50–75. https://doi.org/10.1093/zoolinnean/zlx018

Whitney, J.L., Coleman, R.R. & Deakos, M.H. (2023) Genomic evidence indicates small island-resident populations and sex-biased behaviors of Hawaiian reef manta rays. *BMC Ecology and Evolution*, 23(1), 1–20. https://doi.org/10.1186/s12862-023-02130-0

Williamson, M.J., Tebbs, E.J., Dawson, T.P., Curnick, D.J., Ferretti, F., Carlisle, A.B. et al. (2020) Gap analysis of acoustic tracking data reveals spatial and temporal segregation in sympatric reef sharks. *Research Square Preparation*, 1–17. https://doi.org/10.21203/rs.2.19727/v1

Winterbottom, R. & Anderson, R.C. (1997) A revised checklist of the epipelagic and shore fishes of the Chagos archipelago, Central Indian Ocean. J.L.B. *Smith Institute of Ichthyology. Ichthyological Bulletin*, 66, 1–28.

SUPPORTING INFORMATION

Additional supporting information can be found online in the Supporting Information section at the end of this article.

How to cite this article: Harris, J.L., Hosegood, P., Embling, C.B., Williamson, B.J. & Stevens, G.M.W. (2024). Spatiotemporal variations in reef manta ray (*Mobula alfredi*) residency at a remote meso-scale habitat and its importance in future spatial planning. *Aquatic Conservation: Marine and Freshwater Ecosystems*, 1–20. https://doi.org/10.1002/aqc.4089